

Estimating synchronous changes in condition and density in Eastern Bering Sea fishes

Arnaud Grüss^{1, a*}, Jin Gao^{2, b}, James T. Thorson^{3, c}, Christopher N. Rooper^{4, d}, Grant Thompson^{5, e}, Jennifer L. Boldt^{4, f}, Robert Lauth^{6, g}

¹School of Aquatic and Fishery Sciences, University of Washington, Box 355020, Seattle, WA 98105-5020, USA

²Centre for Fisheries Ecosystem Research, Fisheries and Marine Institute of Memorial University of Newfoundland, 155 Ridge Rd, St. John's, NL A1C 5R3, Canada

³Habitat and Ecosystem Process Research Program, Alaska Fisheries Science Center, National Marine Fisheries Service, NOAA, 7600 Sand Point Way N.E., Seattle, WA 98115, USA

⁴Fisheries and Oceans Canada, Pacific Biological Station, 3190 Hammond Bay Road, Nanaimo, BC, Canada V9T 6N7

⁵Resource Ecology and Fisheries Management Division, Alaska Fisheries Science Center, National Marine Fisheries Service, NOAA, 7600 Sand Point Way N.E., Seattle, WA 98115, USA

⁶Resource Assessment and Conservation Engineering Division, Alaska Fisheries Science Center, National Marine Fisheries Service, NOAA, 7600 Sand Point Way N.E., Seattle, WA 98115, USA

Author email addresses

^agruss.arnaud@gmail.com

^bjin.gao@mi.mun.ca

^cJames.Thorson@noaa.gov

^dChris.Rooper@dfo-mpo.gc.ca

^eGrant.Thompson@noaa.gov

^fJennifer.Boldt@dfo-mpo.gc.ca

^gBob.lauth@noaa.gov

Running Title

Estimating changes in condition and density

Type of article: Research Article

Manuscript length

Abstract (249 words), Manuscript (5,999 words), Literature cited (78)

6 figures, 3 tables

1 appendix and 3 figures appearing in the Electronic supplements

**** Corresponding author***

Dr. Arnaud Grüss

School of Aquatic and Fishery Sciences

University of Washington

Box 355020

Seattle, WA 98105-5020

USA

Telephone: +1 206 543 4270

Email: gruss.arnaud@gmail.com

ABSTRACT: Estimating fish condition, the relative weight of an individual fish given its body length, is an easy way to relate the physiological health and energetic status of fishes to their productivity. Despite evidence of density-dependence effects on condition in some species, previous research has not jointly estimated synchronous changes in condition and density operating at fine spatial scales. Therefore, we developed a spatio-temporal modeling approach that simultaneously estimates correlated variation in density (measured as numbers per area) and condition, where the correlation can be negative (e.g. due to density-dependent competition for food) or positive. We applied our approach to six Eastern Bering Sea (EBS) groundfish species (four flatfishes and two gadoids) for the period 1992-2016, and estimated correlations in spatial variation (persistent patterns) and spatio-temporal variation (short-term patterns). Spatial variation in density had a strong negative effect on spatial variation in condition for the four flatfish species (significant for three species). Spatio-temporal variation in density had a significant negative effect on spatio-temporal variation in condition for two flatfish species. Moreover, for the six study species, bottom temperature was identified as an important predictor of both density and condition. The increasing trend in bottom temperatures between 1992 and 2016 was accompanied by an overall increase in the abundance-weighted condition of five species, including three flatfish species. In conclusion, it will be important to evaluate the impacts of accounting for or ignoring density-dependence and bottom temperature effects on condition within some EBS flatfish assessments (e.g. using a management strategy evaluation framework).

KEY WORDS: Condition, Le Cren's relative condition index, density-dependence, spatio-temporal models, groundfishes, Eastern Bering Sea, bottom temperature effects

1. INTRODUCTION

The physiological health of fishes and their energetic status have been intensively studied to understand and predict their productivity (Wuenschel et al. 2019). Some of the most popular measures of physiology and energetic status include the hepatosomatic index, which determines the status of fish energy reserves by assessing liver weight relative to somatic weight, and the gonadosomatic index, which describes fish maturity by evaluating gonad weight relative to somatic weight (e.g. Lambert & Dutil 1997b, Copeland et al. 2008, Pardoe et al. 2008, Pardoe & Marteinsdóttir 2009). Many studies have also examined muscle and liver energy content or estimated the percent dry weight of muscle and liver (e.g. Love 1958, Kjesbu et al. 1991, Lambert & Dutil 1997a, b, Boldt & Haldorson 2004). However, while physiological methods provide valuable information for studying fish productivity, they are typically logistically challenging and usually rely on a limited number of samples (Wuenschel et al. 2019).

Morphological indices of condition, which express fish weight relative to its length, are ways to relate the physiological health and energetic status of fishes to their productivity (Nash et al. 2006, Boldt et al. 2015). Morphological indices of condition (hereafter simply referred to as “condition indices”) are “integrated measures of physiology for fish populations” that account for fish behavior, life history, environmental and species interactions (Murphy et al. 1990). One of the most employed condition indices is Fulton’s condition factor, which is the ratio of fish weight to the cube of fish length (Lambert & Dutil 1997b, Nash et al. 2006). Another widely used and similar condition index is Le Cren’s relative condition factor (Le Cren 1958), which defines condition as residuals from an allometric length-weight relationship and, therefore, does not impose the relationship between fish length and weight to be cubic (Froese 2006, Pardoe et al. 2008, Thorson 2015).

Condition indices can inform potential survival, reproduction and recruitment successes of fishes. The condition of Pacific herring (*Clupea pallasii*) in Prince William Sound, Alaska was shown to partly influence fish overwintering survival (Paul & Paul 1999). Lambert & Dutil (1997b) discussed that the poor condition of northern Gulf of St. Lawrence cod (*Gadus morhua*) between the late 1980s and the early 1990s may have greatly contributed to the very high mortality rate of the stock, along with overfishing. Other studies similarly found that poor condition may have reduced survival for diverse fish populations (e.g. Love 1958, Wilkins 1967, Krivobok & Tokareva 1972, Newsome & Leduc 1975). Moreover, fishes in poor condition tend to allocate less energy to gonadal development, which may reduce the probability of being mature (e.g. Henderson & Morgan 2002, Henderson & Morgan 2002, Morgan 2004, Dutil et al. 2006) and, therefore, may lower reproduction success. Poor condition can also affect reproduction success by increasing the probability of skipped spawning (Burton et al. 1997, Marshall et al. 1998, Rideout et al. 2000, Jørgensen et al. 2006) or decreasing fecundity (Pinhorn 1984, Kjesbu et al. 1991). Finally, by decreasing total egg production (Marshall & Frank 1999), egg and larval size (Chambers & Leggett 1996, Chambers & Waiwood 1996, Marteinsdottir & Steinarsson 1998) or egg and larval quality (Kjesbu et al. 1992, Chambers & Leggett 1996), poor condition of mature fish may have a negative impact on recruitment success.

Because condition indices provide rich information on potential fish productivity and can be estimated based on large sample sizes, they are valuable for stock and habitat assessments. Many stock assessments are age-structured and employ weight-at-age estimates to convert abundances into biomasses and catches in numbers into catches in biomass. Condition indices can be used to generate time-varying weight-at-age estimates, with the goal to improve the goodness-of-fit of age-structured assessment models to data (Thorson 2015). Moreover, variation in the relationship between reproductive potential and subsequent

recruitment is typically poorly explained (Barrowman & Myers 1996, Francis 1997). By relating reproductive potential to variation in weight-at-length of fishes, condition indices can help fisheries analysts produce more reliable recruitment estimates. For example, condition indices can serve to better quantify the number of batches spawned per year and the number of eggs spawned per batch of the different age classes of mature fish in relation to their weight (Marshall & Frank 1999, Fitzhugh et al. 2012), or the rate at which these different age classes skip spawning (Rideout et al. 2005, Jørgensen et al. 2006). Finally, estimates of spatial variation in condition can be employed in habitat assessments to identify areas where the condition of mature individuals is high during the spawning season and which may, therefore, have disproportionate importance for spawning output. These areas may then be given primary consideration in spatial management plans aiming to protect spawners (Lloret et al. 2002, Grüss et al. 2018).

Spatio-temporal changes in condition and density are expected to take place simultaneously. A large local increase in density may result in decreased condition, due to increased competition for food (e.g. Boxrucker 1987, Pardoe et al. 2008, Thorson 2015). However, in some areas, at least over a certain time period, density and condition may respond similarly to local environmental conditions. For instance, increased local temperatures may boost prey abundance while being optimal for the physiological processes of the species of interest, thereby increasing both local density and condition for this species (Boldt et al. 2015). Thus, it appears important to quantify density-dependence in fish condition over space and time.

Several factors govern physiological and ecological processes, which in turn govern fish condition and density. In particular, bottom temperature was found to influence local density and condition simultaneously in many fish populations (e.g. Michalsen et al. 1998, Hunt et al. 2008, Boldt et al. 2015, Thorson 2015, Laurel et al. 2016). For example, the shift

from sequential cold years to warm years in the Eastern Bering Sea (EBS), Alaska that is responsible for changes in population density distribution in some groundfish species may lead to large changes in spatial overlap with prey, with subsequent effects on groundfish condition (Hunt et al. 2008, Boldt et al. 2015). Specifically, the reduction of the extent of the cold pool (i.e. the area of the EBS with bottom temperatures at or below 2°C) in relatively warm years is accompanied by expansions in the habitat occupied by some groundfish species such as walleye pollock (*Gadus chalcogrammus*). These groundfish species can then access the Middle Shelf of the EBS where the cold pool would usually persist. The increase in the area occupied by the groundfish species may allow for better foraging opportunities, thereby improving groundfish condition (Hunt et al. 2008, Boldt et al. 2015).

In recent years, statistical models that account for spatial and spatio-temporal structure at a fine scale (“spatio-temporal models”) have been increasingly used for informing stock and habitat assessments (Grüss & Thorson 2019, Thorson 2019a). In particular, Thorson (2015) developed the first spatio-temporal model estimating spatio-temporal changes in fish condition, which he applied to California Current groundfishes. This spatio-temporal model was designed to understand how much of the total variation in condition among individuals was explained by covariates (including population density, bottom temperature, and calendar day), temporal variation in condition, spatial variation in condition (i.e. unmeasured variation in condition that is stable over time) and spatio-temporal variation in condition (i.e. unmeasured variation in condition that changes between years). Thorson (2015) found that spatial variation in condition and, to a greater extent, spatio-temporal variation in condition explained a large proportion of total variation among individuals. In this study, we extend the approach of Thorson (2015) by developing the first spatio-temporal model simultaneously estimating spatial and spatio-temporal variation in fish density and Le Cren’s relative condition factor (hereafter simply referred to as “condition”). We apply this spatio-temporal

model to six EBS groundfish species over the period 1992-2016 to answer the following questions: (1) Are correlations between density and condition statistically significant? and (2) Are areas with higher density associated with lower condition (e.g. due to density-dependent competition for food) or greater condition (e.g. because high quality habitat leads to localized concentration of fish while being optimal for fish physiological processes)? We develop alternative spatio-temporal models including or not including bottom temperature effects on density and/or condition, and we then select the most parsimonious model for each groundfish species based on Akaike's information criterion (AIC). Next, we examine correlations between spatial variation in density and spatial variation in condition and between spatio-temporal variation in density and spatio-temporal variation in condition. Finally, we analyze spatio-temporal changes in density and condition in relation to local bottom temperatures where relevant.

2. MATERIALS AND METHODS

2.1. Model specifications

Our spatio-temporal model is a multivariate lognormal generalized linear mixed model (GLMM) which simultaneously estimates spatial and spatio-temporal variation in condition (in units weight per a power-function of length) and numbers-density (in units numbers per area). If we measured density in biomass, then an increase in condition (greater weight per length) would necessarily drive an increase in biomass-density, thus resulting in a positive correlation *ceteris paribus*. To avoid this mechanism generating correlations between density and condition, we measure density in numbers rather than biomass. Our spatio-temporal model is implemented with R package "VAST" release number 3.0.0 (Thorson 2019a), which is publicly available online (<https://github.com/James-Thorson-NOAA/VAST>).

Typically, measurements of fish body weight, W , are assumed to be randomly distributed around an expected body weight that is calculated as an allometric function of body length:

$$\begin{aligned} W &= g(w) \\ w &= \alpha l^\beta \end{aligned} \quad (1)$$

where α is the condition coefficient (with units weight per a power-function of length); β is the allometric coefficient (with dimensionless units); g is a probability distribution that represents unexplained variation in fish body length; and w is predicted body weight (in units kilograms) for a given length l (in units meters). Le Cren's relative condition factor is calculated from the residuals of this allometric relationship (Le Cren 1958). From weight and length data, our spatio-temporal model approximates condition using a log link function and linear predictors, including a Gaussian Markov random field representing spatial variation in condition and another Gaussian Markov random field representing spatio-temporal variation in condition:

$$\log(w(s_i, t_i)) = \delta_w(t_i) + \omega_w(s_i) + \varepsilon_w(s_i, t_i) + \sum_{k=1}^{n_k} \gamma_w(t_i, k) X(s_i, t_i, k) + \beta \log(l_i) \quad (2)$$

where t_i and s_i are, respectively, the year and the location associated with sample i ; $\delta_w(t_i)$ is the intercept for year t_i , which is estimated as a fixed effect; $\omega_w(s_i)$ represents spatial variation in condition and is estimated as a random effect; $\varepsilon_w(s_i, t_i)$ represents spatio-temporal variation in condition and is estimated as a random effect; $X(s_i, t_i, k)$ is an array of n_k measured covariates that explain variation for year t_i and location s_i ; and $\gamma_w(t_i, k)$ is the estimated impact of covariates. Eq. (2) corresponds to Le Cren (1958)'s condition factor equation:

$$\text{Median}(W) = w(s, t) = \exp(\delta_w(t) + \omega_w(s) + \varepsilon_w(s, t) + \sum_{k=1}^{n_k} \gamma_w(t, k) X(s, t, k)) l^\beta \quad (3)$$

such that the intercept $\alpha(s, t) = \exp(\delta_w(t) + \omega_w(s) + \varepsilon_w(s, t) + \sum_{k=1}^{n_k} \gamma_w(t, k)X(s, t, k))$ varies across space and time.

When explaining variation in density (numbers per unit area), we fit a spatio-temporal model to catch data c_i and use a delta-lognormal distribution where the probability of encounter of the species under consideration p and its expected density given encounter (referred to as “positive catch rate”) r are estimated; these two quantities are then multiplied together to yield numbers-density estimates (Lo et al. 1992, Grüss et al. 2019). The delta-lognormal model calculates the probability of catch rate data as:

$$\Pr(c(i) = C) = \begin{cases} 1 - p(i) & \text{if } C = 0 \\ p(i) \times g(C|r(i), \sigma_r^2) & \text{if } C > 0 \end{cases} \quad (4)$$

where probability of encounter, $p(i) = 1 - \exp(-a_i n(s_i, t_i))$, follows a Poisson distribution with intensity equal to the product of local group-densities $n(s_i, t_i)$ and the area sampled a_i , under the assumption that the spatial distribution of aggregations in the neighborhood of sampling is random (Thorson 2018); positive catch rate can be re-expressed as $r(i) = u a_i n(s_i, t_i) / p(i)$, where u is the expected numbers-per-group, which is used to convert between $a_i n(s_i, t_i)$ (the expected number of independently distributed groups or patches) and $r(i)$ (the expected number encountered); $g(C|r(i), \sigma_r^2)$ is the log-normal probability density function for unexplained variation in $c(i)$; and σ_r^2 is residual catch rate variation. Our model approximates local density $n(s_i, t_i)$ similarly to the way it approximates condition:

$$\log(n(s_i, t_i)) = \delta_n(t_i) + \omega_n(s_i) + \varepsilon_n(s_i, t_i) + \sum_{k=1}^{n_k} \gamma_n(t_i, k)X(s_i, t_i, k) \quad (5)$$

We now generalize these two separate models for condition (Eqs. (1-3)) and numbers-density (Eqs. (4-5)) to explain how we can simultaneously estimate both, including their correlation. In effect, our model is provided with both catch rate data and weight and length data, in order to simultaneously approximate two categories of variables, density (category $c = 1$) and condition ($c = 2$):

$$\log(y(s_i, t_i)) = \delta_{c_i}(t_i) + \sum_{f=1}^2 L_{c_i, f}^{(\omega)} \omega_f(s_i) + \sum_{f=1}^2 L_{c_i, f}^{(\varepsilon)} \varepsilon_f(s_i, t_i) \quad (6)$$

$$+ \sum_{k=1}^{n_k} \gamma_{c_i}(t_i, k) X(s_i, t_i, k) + \beta \log(l_i)$$

where $y(s_i, t_i) = n(s_i, t_i)$ and $l_i = 0$ when $c_i = 1$, and $y(s_i, t_i) = w(s_i, t_i)$ when $c_i = 2$; two “factors” for spatial variation ω_f and the associations (i.e. correlations) $L_{c_i, f}^{(\omega)}$ of condition and density with each factor are estimated; and two other “factors” for spatial variation ε_f and the associations $L_{c_i, f}^{(\varepsilon)}$ of condition and density with each factor are also estimated. The matrices $L_{c_i, f}^{(\omega)}$ and $L_{c_i, f}^{(\varepsilon)}$ can serve to calculate correlations between spatial variation in density and spatial variation in condition and between spatio-temporal variation in density and spatio-temporal variation in condition, respectively (Thorson et al. 2016). Thus, the settings of our spatio-temporal model fitted to both catch rate data and weight and length data allow one to determine whether some areas with higher density are associated with lower or greater condition.

More precisely, the spatial variation terms are modeled as Gaussian Markov random fields with correlations over two spatial dimensions and among density and condition (Thorson & Barnett 2017):

$$\text{vec}(\mathbf{\Omega}) \sim \text{GRF}(\mathbf{0}, \mathbf{R} \otimes \mathbf{V}_\omega) \quad (7)$$

where $\mathbf{\Omega}$ is a matrix composed of $\omega_f(s)$ at every location and category of variables (density and condition); \mathbf{R} is a matrix of correlations among locations s , which is calculated from a Matérn function given an estimated decorrelation rate and a transformation matrix representing geometric anisotropy (Thorson et al. 2015); \otimes is the Kronecker product; and \mathbf{V}_ω is the correlation among density and condition:

$$\mathbf{V}_\omega = \mathbf{L}_\omega \mathbf{L}_\omega^T \quad (8)$$

where \mathbf{L}_ω^T is the transpose of \mathbf{L}_ω . Spatio-temporal variation terms are fit independently to each year and are modeled as Gaussian Markov random fields with Matérn covariance, similarly to spatial variation terms (Thorson & Barnett 2017).

2.2. Parameter estimation

All fixed effects of the spatio-temporal model are estimated by identifying the parameter values that maximize the marginal log-likelihood in the R statistical platform (R Core Development Team 2019). The Laplace approximation implemented by R package “TMB” (Kristensen et al. 2016) is employed to compute the marginal log-likelihood through an approximation of the integral across all random effects. TMB uses automatic differentiation to efficiently compute the matrix of second derivatives (which the Laplace approximation employs) and the gradient of the Laplace approximation (which is employed when the fixed effects are maximized). By maximizing the marginal log-likelihood given fixed effects’ maximum likelihood estimates (MLEs), TMB estimates all random effects. In addition, the likelihood of random effects is approximated using the stochastic partial differential equation method (Lindgren et al. 2011), for computational efficiency. Moreover, VAST employs the generalized delta method implemented in TMB to calculate the standard errors of all the fixed and random effects, as well as the standard errors of the derived quantities (Kass & Steffey 1989). We confirm that the spatio-temporal model is converged by checking that the gradient of the marginal log-likelihood is less than 0.0001 for all fixed effects, and that the Hessian matrix of second derivatives of the negative log-likelihood is positive definite.

2.3. Application

We apply our spatio-temporal modeling approach to six groundfish species of the EBS (Fig. 1), including four flatfish species (Kamchatka flounder (*Atheresthes evermanni*), arrowtooth flounder (*Atheresthes stomias*), flathead sole (*Hippoglossoides elassodon*) and yellowfin sole (*Limanda aspera*)), and two gadoids (Pacific cod (*Gadus macrocephalus*) and walleye pollock). These six species are among the species most frequently encountered by fisheries-independent monitoring programs in the EBS region (Stevenson & Hoff 2009). Moreover, walleye pollock is one of the most abundant and socio-economically important fish predators of the North Pacific region (Aydin & Mueter 2007), with an annual harvestable biomass of *ca.* 5 million metric tons and an annual harvested biomass greater than 1.2 million metric tons (Ianelli et al. 2011, 2014). In spite of its relatively small harvested biomass, arrowtooth flounder is also a key species of the EBS, because of its large predatory impacts on commercially important fish species, particularly walleye pollock (Hunsicker et al. 2013, Livingston et al. 2017).

We use the catch rate (in numbers.km⁻²), weight (in g), length (in mm) and temperature (in °C) data collected over the period 1992-2016 during the standardized EBS bottom trawl surveys conducted by NOAA Fisheries' Alaska Fisheries Science Center (Stauffer 2004, Lauth & Conner 2016). These surveys are carried out annually in June-July, employ a fixed-station sampling scheme involving each year approximately 376 stations on a 20 km x 20 km grid (including areas with more dense sampling near significant islands), and sample monitoring stations using a standard trawl net (83-112 eastern otter trawl) for a targeted on-bottom time of 30 minutes at a speed of 1.54 m.s⁻¹. Individual length and weight data are not consistently collected during these surveys; therefore, for each study species, we did not have length and weight data in some years (Table 1).

For the application, we define all spatial and spatio-temporal variation terms over a fixed spatial domain Ω as being piecewise constant, for computation efficiency. To

approximate all the spatial and spatio-temporal variation terms defined over domain Ω , we specify 50 “knots” uniformly distributed over the 20 km x 20 km spatial grid for the EBS, while confirming that our results are qualitatively similar when using more knots. The values of all spatial and spatio-temporal variation terms are tracked at each knot by the spatio-temporal models (Shelton et al. 2014). Consequently, the value of a spatial or spatio-temporal variation term at a given location $s \in \Omega$ is the value of the spatial or spatio-temporal variation term at the knot that is the closest to location s . After having been determined, the locations of the 50 knots is held fixed during model parameter estimation.

However, to be able to produce fine-scale maps, we employ a new “fine-scale” option available in VAST release number 3.0.0 (Thorson 2019b), which follows standard practices of software R-INLA (Lindgren 2012, Lindgren & Rue 2015). This new option allows one to interpolate the predictions of spatio-temporal models from knots j to extrapolation grid cells g , using the triangulated mesh constructed from knots (Lindgren 2012, Lindgren & Rue 2015). Specifically, a matrix \mathbf{M}_g with n_g rows and n_j columns is employed, where each row g has value zero except for three cells that represent the vertices of the triangle containing extrapolation grid cell g . For example, with the fine-scale option, a vector $\boldsymbol{\omega}_f^*$ at all extrapolation grid cells is predicted from values of $\boldsymbol{\omega}_f$ at all n_j knots:

$$\boldsymbol{\omega}_f^* = \mathbf{M}_g \boldsymbol{\omega}_f \quad (9)$$

where vector $\boldsymbol{\omega}_f^*$ has length n_g and contains the predicted value $\boldsymbol{\omega}_f^*(g)$ for spatial variation for every extrapolation grid cell g (Thorson 2019b).

For each study species, we fit four alternative spatio-temporal models: (1) a model without bottom temperature effects; (2) a model with bottom temperature effects on both density and condition; (3) a model with bottom temperature effects on density only; and (4) a model with bottom temperature effects on condition only. We then select the most parsimonious of these four models based on AIC (Akaike 1974). Bottom temperature effects

include the linear effect of bottom temperature (i.e. the effect of T), as well as the quadratic effect of bottom temperature (i.e. the effect of T^2), representing a dome-shaped response of local density and/or condition to local bottom temperatures. Both the T and T^2 covariates were standardized to have a mean of zero and a variance of one prior to being used in the spatio-temporal models; this transformation implies that γX (i.e. a covariate times its coefficient) has a standard deviation equal to γ (Thorson 2015). Next, we use the AIC-selected models to analyze correlations between spatial variation in density and spatial variation in condition and between spatio-temporal variation in density and spatio-temporal variation in condition. Then, for each of the six study species, we examine spatio-temporal changes in density and in condition, in relation to local bottom temperatures where relevant.

Finally, for each study species, we reconstruct trends in abundance-weighted condition z (in g):

$$z(t) = \sum_{g=1}^{n_g} [a_g \times \hat{n}^*(g, t)] \times \hat{\alpha}^*(g, t) \quad (10)$$

where a_g is the surface area (in km²) associated with extrapolation grid cell g ; $\hat{n}^*(g, t)$ is the smoothed density estimated for extrapolation grid cell g in year t (in numbers.km⁻²); and $\hat{\alpha}^*(g, t)$ is the smoothed condition estimated for extrapolation grid cell g in year t (in g). Since this is the first time that an abundance-weighted estimate is generated with R package “VAST”, we also compare results with a simplified estimator (see Appendix S2 for details and results).

3. RESULTS

We fitted four alternative spatio-temporal models for each of the six study species (i.e. a total of 24 spatio-temporal models). The AIC-selected model (i.e. most parsimonious model) of all study species included bottom temperature effects on both density and condition

(Table 2), in addition to spatial variation in density condition (i.e. unmeasured variation in density and condition that is stable over time) and spatio-temporal variation in density and condition (i.e. unmeasured variation in density condition that changes between years).

For all study species except walleye pollock, spatial variation in density was negatively correlated with spatial variation in condition (Fig. 2a). The correlation between spatial variation in density and spatial variation in condition was significant for three flatfish species: Kamchatka flounder, arrowtooth flounder and yellowfin sole (two-sided Wald test, $p < 0.001$ for all three species). The mean correlation coefficient between spatial variation in density and spatial variation in condition of the fourth study flatfish species, flathead sole, was strongly negative; however, this mean correlation coefficient was not significant, because of its very large standard errors (Fig. 2a; two-sided Wald test, $p = 0.38$).

The correlation between spatio-temporal variation in density and spatio-temporal variation in condition was negative and significant for two of the four study flatfish species (Fig. 2b): arrowtooth flounder (two-sided Wald test, $p = 0.01$), and flathead sole (two-sided Wald test, $p = 0.04$). By contrast, the correlation coefficient between spatio-temporal variation in density and spatio-temporal variation in condition of Kamchatka flounder, yellowfin sole, Pacific cod and walleye pollock was positive and not significant.

For all study species, the linear and quadratic effects of bottom temperature on density and condition were usually significant (Table 3). The exceptions to this usual pattern were the linear effect of bottom temperature on walleye pollock density, the quadratic effect of bottom temperature on Pacific cod density, and the quadratic effect of bottom temperature on flathead sole condition. For all species, the linear effects of bottom temperature on density and condition were positive, while the quadratic effects were usually negative (except for Kamchatka flounder density, arrowtooth flounder density, and flathead sole condition; Table

3). This entails that it was usually possible to identify the optimal bottom temperature for population density and fish condition for the six study species (Table 3).

We examine here in detail the patterns of spatial and spatio-temporal variation in density and condition only for Kamchatka flounder, arrowtooth flounder and yellowfin sole for select years (Figs. 3-5), including 1999 and 2012, which were very cold years, and 2016, which was a very warm year (Fig. S1). All the spatial and spatio-temporal variation estimates of the study species for the years of the period 1992-2016 for which both catch rate and length-weight data were available are provided in the Electronic supplements (Fig. S3).

The expected density of Kamchatka flounder was highest on the Outer Shelf of the EBS, where the expected condition of the species was lowest (Figs. 3a-b). The expected condition for Kamchatka flounder was highest on the Inner Shelf of the EBS (Fig. 3b). In the very cold year of 2012, arrowtooth flounder density and condition over the entire EBS were lower than their long-term average, although condition was relatively higher than average in the central part of the Outer Shelf than elsewhere in the EBS region (Figs. 4c-d). In the very warm year of 2016, arrowtooth flounder density was higher than its long-term average on the Inner Shelf, where condition was relatively lower than average (Figs. 4e-f). In 2016, arrowtooth flounder condition was higher than its long-term in the northern and central parts of the Outer Shelf of the EBS (Fig. 4f).

As was the case for Kamchatka flounder, the expected density of arrowtooth flounder was highest on the Outer Shelf of the EBS, where its expected condition was low; and the Inner Shelf was the area of the EBS where the highest values of arrowtooth flounder expected condition occurred (Figs. 4a-b). In the very cold year of 2012, arrowtooth flounder density and condition tended to be lower than their long-term averages over the entire EBS, although condition was relatively higher than average in the central part of the Outer Shelf than elsewhere in the EBS region (Figs. 4c-d). In the very warm year of 2016, arrowtooth flounder

density was higher than its long-term average on the Inner Shelf, where the condition of the species was lower than average (Figs. 4e-f). In 2016, arrowtooth flounder condition was higher than its long-term average in the northern and central parts of the Outer Shelf of the EBS (Fig. 4f).

The expected density of yellowfin sole was highest on the Inner and Middle Shelf, where the expected condition of the species was lowest (Figs. 5a-b). The highest values of yellowfin sole expected condition were found in the southern part of the Outer Shelf of the EBS (Fig. 5b). In the very cold year of 1999, yellowfin sole density was higher than its long-term average in the northernmost areas of the EBS, contrasting with the rest of the EBS region where the density of the species tended to be lower than average (Figs. 5c-d). In 1999, yellowfin condition was lower than its long-term average on the Inner Shelf (Fig. 5d). In the very warm year of 2016, yellowfin sole density was higher than its long-term average in the southern part of the Outer Shelf, while the condition of the species was higher than average on the Inner Shelf and in the northern part of the Middle Shelf (Figs. 5e-f).

Because the spatio-temporal models estimated near-exact opposite patterns of spatial variation in density and spatial variation in condition for Kamchatka flounder, arrowtooth flounder and yellowfin sole (Figs. 3-5), we conducted additional analyses to determine whether estimating density and condition jointly (i.e. assuming a correlation between the two variables) vs. separately (i.e. not assuming a correlation) would yield different results (Fig. S4). For flathead sole, Pacific cod and Walleye pollock, the patterns of spatial variation in condition were virtually unchanged when density and condition were estimated jointly vs. separately. By contrast, for Kamchatka flounder, arrowtooth flounder and yellowfin sole, the spatio-temporal model estimating density and condition jointly shrank spatial variation in condition somewhat towards the inverse of the spatial variation in density, yet patterns of

spatial variation in condition were qualitatively similar with or without correlation between density and condition (Fig. S4).

None of the time series of abundance-weighted condition showed a continuous increasing or decreasing trend, except that of Kamchatka flounder (Fig. 6). The time series of abundance-weighted condition of Kamchatka flounder demonstrated a marked increasing trend between 1992 and 2016. Moreover, the abundance-weighted condition of arrowtooth flounder increased between 1992 and 2005 and tended to decrease afterwards. By contrast, the abundance-weighted condition of walleye pollock decreased between 1992 and 2009 and largely increased afterwards. Between 1992 and 2016, the abundance-weighted condition of five species (Kamchatka flounder, arrowtooth flounder, flathead sole, Pacific cod, and walleye pollock) increased, while that of yellowfin sole showed virtually no change. In the very cold year of 1999 (the coldest year of the period 1992-2016; Fig. S1), the abundance-weighted condition of five of the six study species (Kamchatka flounder, arrowtooth flounder, flathead sole, yellowfin sole, and Pacific cod) was at or near its lowest level, and that of walleye pollock was also relatively low. In the very warm year of 2016 (the warmest year of the period 1992-2016; Fig. S1), the abundance-weighted condition of four of the six study species (Kamchatka flounder, flathead sole, yellowfin sole, and walleye pollock) was at or near its highest level, and that of arrowtooth flounder and Pacific cod was also relatively high (Fig. 6).

4. DISCUSSION

Fish density can influence multiple life history processes, including natural mortality, growth, reproduction and recruitment, with important consequences for resource management decisions (Stearns & Crandall 1984, Sánchez Lizaso et al. 2000, Forrest et al. 2013).

However, modeling studies aiming to support resource management have generally only

considered density-dependent effects on recruitment (Grüss et al. 2012, Andersen et al. 2017). Moreover, although there is growing research interest in measuring density dependence in growth (e.g. Lorenzen & Enberg 2002, Lorenzen 2016), this density dependence is generally not measured at fine spatial scales. In this study, we developed the first spatio-temporal statistical modeling approach simultaneously estimating changes in density and condition at fine spatial scales, which allows for the evaluation of the effects of density on fish condition. The application of our approach to six EBS groundfish species showed that it is important to evaluate the impacts of accounting for or ignoring density-dependence effects on condition in the assessments of some flatfish species (e.g. using a management strategy evaluation framework; Punt et al. 2016). Specifically, we found that: (1) unmeasured variation in density that is stable over time (i.e. spatial variation in density) had a significant and strongly negative effect on unmeasured variation in condition that is stable over time (i.e. spatial variation in condition) for three of the four study flatfish species; and (2) unmeasured variation in density that changes between years (i.e. spatio-temporal variation in density) had a negative and significant effect on unmeasured variation in condition that changes between years (i.e. spatio-temporal variation in condition) for two of the four study flatfish species.

We found that density-dependent changes in condition were more prevalent for flatfishes than for gadoids in the EBS. We also found that, in the EBS region, the influence of spatial variation in density on spatial variation in condition was stronger than the influence of spatio-temporal variation in density on spatio-temporal variation in condition. We initially expected density to have a stronger effect on the condition of EBS gadoids, based on empirical studies conducted in other marine regions (e.g. Lambert & Dutil 1997b, Marshall & Frank 1999, Pardoe et al. 2008). We also initially expected that spatio-temporal variation in condition would be more strongly impacted by changes in density than spatial variation in condition, based on the results from Thorson (2015) for the California Current, one of the

world's major upwelling systems. We suspect that our two above-mentioned findings for the EBS are due to the fact that benthic production, which is more stable and lower over time than pelagic production, is more important in the EBS than in other marine regions like the California Current (McConnaughey & Smith 2000, Hunt et al. 2008).

We also found that bottom temperature had large effects on both density and condition for the six study species. First, the most parsimonious spatio-temporal model of all study species included bottom temperature effects on both density and condition. Then, the tendency for bottom temperatures to increase between the first (1992) and last year (2016) of the study period (Fig. S1) was accompanied by an overall increase in the abundance-weighted condition of five of the six study species (Kamchatka flounder, arrowtooth flounder, flathead sole, Pacific cod, and walleye pollock) (Fig. 6). Finally, we found that the coldest and warmest years of the period 1992-2016 (1999 and 2016, respectively) were associated with, respectively, low and high fish condition for all study species, as shown previously by Boldt et al. (2015). Boldt et al. (2015) discussed that low fish conditions in the EBS in 1999 were likely due to the fact that low bottom temperatures reduced both prey productivity and predator-prey spatial overlap, while also increasing predator energy requirements. Therefore, we conclude that forecasts of changes in weight-at-age within some EBS flatfish assessments will require understanding both density-dependence and bottom temperature effects on condition.

Local patterns of spatial and spatio-temporal variation in density and condition generally varied largely from one study species to another (Figs. 3-5 and Fig. S3). Exceptions to this general pattern included Kamchatka flounder and arrowtooth flounder, whose patterns of spatial and spatio-temporal variation in density and condition were similar (Figs. 3-4 and Fig. S3). This result is not surprising, as Kamchatka flounder and arrowtooth flounder share very similar biological and ecological attributes (Stevenson & Hoff 2009). However, while

the local patterns of spatial and spatio-temporal variation in density and condition of Kamchatka flounder and arrowtooth flounder were similar, the abundance-weighted condition of the Kamchatka flounder population increased markedly over the period 1992-2016, while that of the arrowtooth flounder population increased until 2005 and tended to decrease afterwards. Interestingly, the abundance-weighted condition of the walleye pollock population followed opposite trends to that of the arrowtooth flounder population, namely decreased until 2009 and then largely increased. This result may stem from the fact that arrowtooth flounder is the major predator of walleye pollock, so that a reduction in arrowtooth flounder condition may decrease the level of predation pressure exerted by the arrowtooth flounder population on walleye pollock, thereby allowing for an increase in walleye pollock condition (Hunsicker et al. 2013, Livingston et al. 2017). We also suspect that introducing arrowtooth flounder density as a covariate in the spatio-temporal model of walleye pollock may result in a more parsimonious and more reliable model.

We envision three main avenues for future research. First, because the spatial distribution patterns of the juveniles and adults of most fish species are distinct, spatio-temporal models should ideally be developed separately for juveniles and adults for estimating simultaneous changes in condition and density. Second, one could conduct multi-species analyses using a more complex spatio-temporal model estimating spatial and spatio-temporal variation in density and condition for multiple species simultaneously (or for the juvenile and adult stages of multiple species simultaneously, if data availability allows) (Thorson & Barnett 2017). This more complex spatio-temporal model would employ a similar model structure (i.e. Eq. 6), but would associate each category c with a unique combination of species and variable (e.g. $c = 1$ and $c = 2$ would be density and condition for Kamchatka flounder, $c = 3$ and $c = 4$ would be density and condition for arrowtooth flounder, etc.). Multi-species analyses using the more complex spatio-temporal model would allow one to infer

results for specific guilds (e.g. small-mouth vs. predatory flatfishes), but also to estimate spatial and spatio-temporal variation in density and condition for species with few encounter data (which single-species spatio-temporal models are not able to do) (Thorson & Barnett 2017). Finally, in the present study, we considered only the effects of bottom temperatures on density and condition, but future studies may include more covariates in spatio-temporal models and evaluate which covariates have the strongest effects on density and condition (Thorson 2015). In this study, we allowed for linear and quadratic bottom temperature effects, but future studies could also consider spatially-varying coefficients to explore non-local effects of oceanographic indices such as the cold pool. Previous studies have shown that these oceanographic indices have a large impact on spatial distribution for demersal species in the EBS (Hunt et al. 2011, Hollowed et al. 2012), but they have not to our knowledge been applied in spatial models of fish condition.

In conclusion, our novel spatio-temporal modeling approach for simultaneously estimating changes in density and condition highlighted the need to evaluate the impacts of accounting for or ignoring density-dependence and bottom temperature effects on condition within some EBS flatfish assessments (e.g. using a management strategy evaluation framework). We recommend future studies to implement our approach to diverse marine ecosystems and to more species to better inform stock and habitat assessments (Marshall & Frank 1999, Lloret et al. 2002, Thorson 2015), but also to answer important ecological questions, such as the contribution of decreases in fish condition to marine population collapses (e.g. northern Gulf of St. Lawrence cod; Lambert & Dutil 1997b) or the impacts of density-dependent changes in condition on population biomasses and fisheries yields relative to those of density-dependent changes in recruitment (Andersen et al. 2017).

Acknowledgments. The present work was funded by the Habitat Information for Stock Assessments program [grant number 17-034]. We are very grateful to Franz Mueter for his contribution to the proposal that funded this work, and to Tim Essington for insightful comments on an earlier version of the manuscript. The scientific results and conclusions, as well as any views or opinions expressed herein, are those of the authors and do not necessarily reflect those of NOAA or the Department of Commerce.

Electronic supplements

Fig. S1. Maps showing the bottom temperature estimates (in °C) used within the spatio-temporal models to approximate spatial and spatio-temporal variation in density and condition, for each year of the period 1992-2016.

Appendix S2. Details and predictions of the simplified estimator.

Fig. S3. Spatial variation in log-density and log-condition and spatio-temporal variation in log-density and log-condition for different years of the period 1992-2016, for the Akaike's information criterion (AIC)-selected models of the six study species. The color legends for spatio-temporal variation in log-density and log-condition are provided in the rightmost columns and have units $\ln(\text{abundance} \cdot \text{km}^{-2})$ in the case of log-density and $\ln(g)$ in the case of log-condition. For each species, only estimations for those years where both density and length-weight data were available are shown.

Fig. S4. Spatial variation in log-condition (in $\ln(g)$) predicted by the Akaike's information criterion (AIC)-selected models of the six study species, when density and condition are estimated jointly vs. separately.

LITERATURE CITED

- Akaike H (1974) A new look at statistical-model identification. *IEEE Trans Automat Contr* 19:716–723.
- Andersen KH, Jacobsen NS, Jansen T & Beyer JE (2017) When in life does density dependence occur in fish populations? *Fish Fish* 18:656–667.
- Aydin K, Mueter F (2007) The Bering Sea—A dynamic food web perspective. *Deep Sea Res Part 2 Top Stud Oceanogr* 54:2501–2525.
- Barrowman NJ, Myers RA (1996) Is fish recruitment related to spawner abundance? *Fish Bull* 94:707–724.
- Boldt J, Rooper C, Hoff J (2015) Eastern Bering Sea Groundfish Condition. In: Zador S (ed) *Ecosystem Considerations 2015 Status of Alaska's Marine Ecosystems*. North Pacific Fishery Management Council, Anchorage, AK, p 182–190
- Boldt JL, Haldorson LJ (2004) Size and condition of wild and hatchery pink salmon juveniles in Prince William Sound, Alaska. *Trans Am Fish Soc* 133:173–184.
- Boxrucker J (1987) Largemouth Bass Influence on Size Structure of Crappie Populations in Small Oklahoma Impoundments. *N Am J Fish Manag* 7:273–278.
- Burton MP, Penney RM, Biddiscombe S (1997) Time course of gametogenesis in Northwest Atlantic cod (*Gadus morhua*). *Can J Fish Aquat Sci* 54:122–131.
- Chambers RC, Leggett WC (1996) Maternal Influences on Variation in Egg Sizes in Temperate Marine Fishes. *Integr Comp Biol* 36:180–196.
- Chambers RC, Waiwood KG (1996) Maternal and seasonal differences in egg sizes and spawning characteristics of captive Atlantic cod, *Gadus morhua*. *Can J Fish Aquat Sci* 53:1986–2003.
- Copeland T, Murphy BR, Ney JJ (2008) Interpretation of relative weight in three populations of wild bluegills: a cautionary tale. *N Am J Fish Manag* 28:368–377.
- Dutil J-D, Godbout G, Blier PU, Groman D (2006) The effect of energetic condition on growth dynamics and health of Atlantic cod (*Gadus morhua*). *J Appl Ichthyol* 22:138–144.
- Fitzhugh GR, Shertzer KW, Kellison GT, Wyanski DM (2012) Review of size- and age-dependence in batch spawning: implications for stock assessment of fish species exhibiting indeterminate fecundity. *Fish Bull* 110:413–425.
- Forrest RE, McAllister MK, Martell SJ & Walters CJ (2013) Modelling the effects of density-dependent mortality in juvenile red snapper caught as bycatch in Gulf of Mexico shrimp fisheries: Implications for management. *Fish Res* 146:102–120.
- Francis R (1997) Comment: How should fisheries scientists and managers react to uncertainty about stock-recruit relationships? *Can J Fish Aquat Sci* 54:982–983.
- Froese R (2006) Cube law, condition factor and weight–length relationships: history, meta-analysis and recommendations. *J Appl Ichthyol* 22:241–253.
- Grüss A, Biggs C, Heyman WD, Erisman B (2018) Prioritizing monitoring and conservation efforts for fish spawning aggregations in the US Gulf of Mexico. *Sci Rep* 8:8473.

- Grüss A, Kaplan DM & Lett C (2012) Estimating local settler–recruit relationship parameters for complex spatially explicit models. *Fish Res* 127:34–39.
- Grüss A, Thorson JT (2019) Developing spatio-temporal models using multiple data types for evaluating population trends and habitat usage. *ICES J Mar Sci*, doi: 10.1093/icesjms/fsz075
- Grüss A, Walter III JF, Babcock EA, Forrestal FC, Thorson JT, Laretta MV, Schirripa MJ (2019) Evaluation of the impacts of different treatments of spatio-temporal variation in catch-per-unit-effort standardization models. *Fish Res* 213:75–93.
- Henderson BA, Morgan GE (2002) Maturation of walleye by age, size and surplus energy. *J Fish Biol* 61:999–1011.
- Hollowed AB, Barbeaux SJ, Cokelet ED, Farley E, Kotwicki S, Ressler PH, Spital C, Wilson CD (2012) Effects of climate variations on pelagic ocean habitats and their role in structuring forage fish distributions in the Bering Sea. *Deep Sea Res Part 2 Top Stud Oceanogr* 65:230–250.
- Hunsicker ME, Ciannelli L, Bailey KM, Zador S, Stige LC (2013) Climate and Demography Dictate the Strength of Predator-Prey Overlap in a Subarctic Marine Ecosystem. *PLoS ONE* 8:e66025.
- Hunt GL, Coyle KO, Eisner LB, Farley EV, Heintz RA, Mueter F, Napp JM, Overland JE, Ressler PH, Salo S (2011) Climate impacts on eastern Bering Sea foodwebs: a synthesis of new data and an assessment of the Oscillating Control Hypothesis. *ICES J Mar Sci* 68:1230–1243.
- Hunt GL, Stabeno PJ, Strom S, Napp JM (2008) Patterns of spatial and temporal variation in the marine ecosystem of the southeastern Bering Sea, with special reference to the Pribilof Domain. *Deep Sea Res Part 2 Top Stud Oceanogr* 55:1919–1944.
- Ianelli JN, Honkalehto T, Barbeaux S, Kotwicki S (2014) Chapter 1: Assessment of the walleye pollock stock in the Eastern Bering Sea. In: *Stock Assessment and Fishery Evaluation Report for the Groundfish Resources of the Bering Sea/ Aleutian Islands Regions*. Alaska Fisheries Science Center, National Marine Fisheries Service, Anchorage, AK, p 55–156
- Ianelli JN, Honkalehto T, Barbeaux S, Kotwicki S, Aydin K, Williamson N (2011) Assessment of the walleye pollock stock in the Eastern Bering Sea. In: *Stock assessment and fishery evaluation report for the groundfish resources of the Bering Sea/Aleutian Islands regions*. Alaska Fisheries Science Center, National Marine Fisheries Service, Seattle, WA, p 51–168
- Jørgensen C, Ernande B, Fiksen Ø, Dieckmann U (2006) The logic of skipped spawning in fish. *Can J Fish Aquat Sci* 63:200–211.
- Kass RE, Steffey D (1989) Approximate Bayesian inference in conditionally independent hierarchical models (parametric empirical Bayes models). *J Am Stat Assoc* 84:717–726.
- Kjesbu OS, Klungsøyr J, Kryvi H, Witthames PR, Walker MG (1991) Fecundity, Atresia, and Egg Size of Captive Atlantic Cod (*Gadus morhua*) in Relation to Proximate Body Composition. *Can J Fish Aquat Sci* 48:2333–2343.
- Kjesbu OS, Kryvi H, Sundby S, Solemdal P (1992) Buoyancy variations in eggs of Atlantic cod (*Gadus morhua* L.) in relation to chorion thickness and egg size: theory and observations. *J Fish Biol* 41:581–599.
- Kristensen K, Nielsen A, Berg CW, Skaug H, Bell B (2016) TMB: automatic differentiation and Laplace approximation. *J Stat Softw* 70:1–20.
- Krivobok MN, Tokareva GI (1972) Dynamics of weight variations of the body and individual organs of the Baltic cod during the maturation of gonads. *Trudy VNIRO*, 85:45–55.

- Lambert Y, Dutil J-D (1997a) Can simple condition indices be used to monitor and quantify seasonal changes in the energy reserves of cod (*Gadus morhua*)? *Can J Fish Aquat Sci* 54:104–112.
- Lambert Y, Dutil J-D (1997b) Condition and energy reserves of Atlantic cod (*Gadus morhua*) during the collapse of the northern Gulf of St. Lawrence stock. *Can J Fish Aquat Sci* 54:2388–2400.
- Laurel BJ, Spencer M, Iseri P, Copeman LA (2016) Temperature-dependent growth and behavior of juvenile Arctic cod (*Boreogadus saida*) and co-occurring North Pacific gadids. *Polar Biol* 39:1127–1135.
- Lauth RR, Conner J (2016) Results of the 2013 eastern Bering Sea continental shelf bottom trawl survey of groundfish and invertebrate resources. NOAA Technical Memorandum No. NMFS-AFSC-331. Seattle, WA.
- Le Cren ED (1958) Observation on the growth of perch (*Perca fluviatilis* L.) over twenty-two years with special reference to the effects of temperature and changes in population density. *J Anim Ecol* 27:287–334.
- Lindgren F (2012) Continuous domain spatial models in R-INLA. *The ISBA Bulletin* 19:14–20.
- Lindgren F, Rue H (2015) Bayesian spatial modelling with R-INLA. *J Stat Softw* 63:1–25.
- Lindgren F, Rue H, Lindström J (2011) An explicit link between Gaussian fields and Gaussian Markov random fields: the stochastic partial differential equation approach. *J R Stat Soc Series B* 73:423–498.
- Livingston PA, Aydin K, Buckley TW, Lang GM, Yang M-S, Miller BS (2017) Quantifying food web interactions in the North Pacific – a data-based approach. *Environ Biol Fish* 100:443–470.
- Lloret J, Gil de Sola L, Souplet A, Galzin R (2002) Effects of large-scale habitat variability on condition of demersal exploited fish in the north-western Mediterranean. *ICES J Mar Sci* 59:1215–1227.
- Lo NC, Jacobson LD, Squire JL (1992) Indices of relative abundance from fish spotter data based on delta-lognormal models. *Can J Fish Aquat Sci* 49:2515–2526.
- Lorenzen K (2016) Toward a new paradigm for growth modeling in fisheries stock assessments: embracing plasticity and its consequences. *Fish Res* 180:4–22.
- Lorenzen K, Enberg K (2002) Density-dependent growth as a key mechanism in the regulation of fish populations: evidence from among-population comparisons. *Proc R Soc Lond B Biol Sci* 269:49–54.
- Love RM (1958) Studies on the north sea cod. III.—Effects of starvation. *J Sci Food Agric* 9:617–620.
- Marshall CT, Frank KT (1999) The effect of interannual variation in growth and condition on haddock recruitment. *Can J Fish Aquat Sci* 56:347–355.
- Marshall CT, Kjesbu OS, Yaragina NA, Solemdal P, Ulltang Ø (1998) Is spawner biomass a sensitive measure of the reproductive and recruitment potential of Northeast Arctic cod? *Can J Fish Aquat Sci* 55:1766–1783.
- Marteinsdottir G & Steinarsson A (1998) Maternal influence on the size and viability of Iceland cod *Gadus morhua* eggs and larvae. *J Fish Biol* 52:1241–1258.
- McConnaughey RA, Smith KR (2000) Associations between flatfish abundance and surficial sediments in the eastern Bering Sea. *Can J Fish Aquat Sci* 57:2410–2419.
- Michalsen K, Ottersen G, Nakken O (1998) Growth of North-east Arctic cod (*Gadus morhua* L.) in relation to ambient temperature. *ICES J Mar Sci* 55:863–877.
- Morgan MJ (2004) The relationship between fish condition and the probability of being mature in American plaice (*Hippoglossoides platessoides*). *ICES J Mar Sci* 61:64–70.

- Murphy BR, Brown ML, Springer TA (1990) Evaluation of the Relative Weight (W_r) Index, with New Applications to Walleye. *N Am J Fish Manag* 10:85–97.
- Nash RDM, Valencia AH, Geffen AJ (2006) The Origin of Fulton’s Condition Factor—Setting the Record Straight. *Fisheries* 31:236–238.
- Newsome GE, Leduc G (1975) Seasonal Changes of Fat Content in the Yellow Perch (*Perca flavescens*) of Two Laurentian Lakes. *J Fish Res Bd Can* 32:2214–2221.
- Pardoe H, Marteinsdóttir G (2009) Contrasting trends in two condition indices: bathymetric and spatial variation in autumn condition of Icelandic cod *Gadus morhua*. *J Fish Biol* 75:282–289.
- Pardoe H, Thórdarson G, Marteinsdóttir G (2008) Spatial and temporal trends in condition of Atlantic cod *Gadus morhua* on the Icelandic shelf. *Mar Ecol Prog Ser* 362:261–277.
- Paul AJ, Paul JM (1999) Interannual and regional variations in body length, weight and energy content of age-0 Pacific herring from Prince William Sound, Alaska. *J Fish Biol* 54:996–1001.
- Pinhorn AT (1984) Temporal and spatial variation in fecundity of Atlantic cod (*Gadus morhua*) in Newfoundland waters. *J Northwest Atl Fish Sci* 5:161–170.
- Punt AE, Butterworth DS, de Moor CL, De Oliveira JA, Haddon M (2016) Management strategy evaluation: best practices. *Fish Fish* 17:303–334.
- R Core Development Team (2019) R: A Language and Environment for Statistical Computing. R Foundation for Statistical Computing, Vienna, Austria. <http://www.R-project.org/>.
- Rideout RM, Burton MPM, Rose GA (2000) Observations on mass atresia and skipped spawning in northern Atlantic cod, from Smith Sound, Newfoundland. *J Fish Biol* 57:1429–1440.
- Rideout RM, Rose GA, Burton MPM (2005) Skipped spawning in female iteroparous fishes. *Fish Fish* 6:50–72.
- Sánchez Lizaso J, Goñi R, Reñones O, Charton JG, Galzin R, Bayle JT, Jerez PS, Ruzafa AP & Ramos AA (2000) Density dependence in marine protected populations: a review. *Environ Conserv* 27:144–158.
- Shelton AO, Thorson JT, Ward EJ, Feist BE (2014) Spatial semiparametric models improve estimates of species abundance and distribution. *Can J Fish Aquat Sci* 71:1655–1666.
- Stauffer G (2004) NOAA Protocols for Groundfish Bottom Trawl Surveys of the Nation’s Fishery Resources. U.S. Department of Commerce, NOAA Technical Memorandum NMFS-F/SPO-65, 205 p
- Stearns SC & Crandall RE (1984) Plasticity for age and size at sexual maturity: a life-history response to unavoidable stress. In: Potts GW, Wootton RJ (eds) *Fish Reproductive Strategies and Tactics*. Academic Press, New York, NY, p 13–30
- Stevenson DE, Hoff GR (2009) Species identification confidence in the eastern Bering Sea shelf survey (1982-2008). AFSC Processed Report 2009-04. Alaska Fisheries Science Center, NOAA, National Marine Fisheries Service, Seattle, WA, 46 p
- Thorson JT (2019) Guidance for decisions using the Vector Autoregressive Spatio-Temporal (VAST) package in stock, ecosystem, habitat and climate assessments. *Fish Res* 210:143–161.
- Thorson JT (2015) Spatio-temporal variation in fish condition is not consistently explained by density, temperature, or season for California Current groundfishes. *Mar Ecol Prog Ser* 526:101–112.
- Thorson JT (2018) Three problems with the conventional delta-model for biomass sampling data, and a computationally efficient alternative. *Can J Fish Aquat Sci* 75:1369–1382.
- Thorson JT (2019b) VAST model structure and user interface. 24 p

- Thorson JT, Barnett LA (2017) Comparing estimates of abundance trends and distribution shifts using single-and multispecies models of fishes and biogenic habitat. *ICES J Mar Sci* 74:1311–1321.
- Thorson JT, Ianelli JN, Larsen EA, Ries L, Scheuerell MD, Szuwalski C, Zipkin EF (2016) Joint dynamic species distribution models: a tool for community ordination and spatio-temporal monitoring. *Glob Ecol Biogeogr* 25:1144–1158.
- Thorson JT, Shelton AO, Ward EJ, Skaug HJ (2015) Geostatistical delta-generalized linear mixed models improve precision for estimated abundance indices for West Coast groundfishes. *ICES J Mar Sci* 72:1297–1310.
- Wilkins NP (1967) Starvation of the herring, *Clupea harengus* L.: Survival and some gross biochemical changes. *Comp Biochem Physiol* 23:503–518.
- Wuenschel MJ, McElroy WD, Oliveira K, McBride RS (2019) Measuring fish condition: an evaluation of new and old metrics for three species with contrasting life histories. *Can J Fish Aquat Sci* 76:886–903.

<https://github.com/James-Thorson-NOAA/VAST>

TABLES

Table 1. Study species, and years for which both density and length-weight data are available for these species.

Species	Years for which both density and length-weight data are available for the species
Kamchatka flounder (<i>Atheresthes evermanni</i>)	1995-1997, 2002, 2012-2016
Arrowtooth flounder (<i>Atheresthes stomias</i>)	1996, 2002, 2004-2006, 2008-2012, 2014-2016
Flathead sole (<i>Hippoglossoides elassodon</i>)	1997, 1999-2016
Yellowfin sole (<i>Limanda aspera</i>)	1994, 1999-2016
Pacific cod (<i>Gadus macrocephalus</i>)	1993, 1998-2016
Walleye pollock (<i>Gadus chalcogrammus</i>)	1999-2016

Table 2. Model selection results using Akaike’s information criterion (AIC) applied to the maximum marginal likelihood for each of the spatio-temporal models fitted in this study.

Species	ΔAIC for the model without bottom temperature effects	ΔAIC for the model with bottom temperature effects on both density and condition	ΔAIC for the model with bottom temperature effects on density only	ΔAIC for the model with bottom temperature effects on condition only
Kamchatka flounder	442.8	0	226.6	211.9
Arrowtooth flounder	398.7	0	508.9	523.9
Flathead sole	383.1	0	12	369.9
Yellowfin sole	1256.8	0	398.1	835
Pacific cod	1189.2	0	220.1	352.6
Walleye pollock	928.8	0	643.4	284.3

Table 3. Linear and quadratic bottom temperature effects on density and condition predicted by the Akaike’s information criterion (AIC)-selected spatio-temporal models of the six study species, and predicted optimal bottom temperatures for density and condition for the six species. *P*-values for a two-sided Wald test (strength-of-evidence measures of importance) are also indicated in parentheses.

Species	Linear effect of bottom temperature on density	Quadratic effect of bottom temperature on density	Optimal bottom temperature for density (°C)	Linear effect of bottom temperature on condition	Quadratic effect of bottom temperature on condition	Optimal bottom temperature for condition (°C)
Kamchatka flounder	0.18 ± 0.03 (<i>p</i> < 0.001)	0.17 ± 0.03 (<i>p</i> < 0.001)	Not applicable	40.82 ± 0.70 (<i>p</i> < 0.001)	-39.79 ± 1.29 (<i>p</i> < 0.001)	1.1
Arrowtooth flounder	0.41 ± 0.04 (<i>p</i> < 0.001)	0.13 ± 0.03 (<i>p</i> < 0.001)	Not applicable	40.82 ± 0.70 (<i>p</i> < 0.001)	-39.79 ± 1.29 (<i>p</i> < 0.001)	0.5
Flathead sole	0.14 ± 0.06 (<i>p</i> = 0.02)	-0.12 ± 0.02 (<i>p</i> < 0.001)	0.6	0.14 ± 0.06 (<i>p</i> = 0.02)	0.002 ± 0.03 (<i>p</i> = 0.94)	Not applicable
Yellowfin sole	0.91 ± 0.05 (<i>p</i> < 0.001)	-0.18 ± 0.04 (<i>p</i> < 0.001)	2.5	6.60 ± 0.21 (<i>p</i> < 0.001)	-1.25 ± 0.09 (<i>p</i> < 0.001)	2.6
Pacific cod	0.15 ± 0.03 (<i>p</i> < 0.001)	-0.01 ± 0.02 (<i>p</i> = 0.74)	9.9	53.40 ± 0.49 (<i>p</i> < 0.001)	-23.16 ± 0.43 (<i>p</i> < 0.001)	1.2
Walleye pollock	0.02 ± 0.03 (<i>p</i> = 0.55)	-0.12 ± 0.02 (<i>p</i> < 0.001)	0.1	11.14 ± 0.79 (<i>p</i> < 0.001)	-3.65 ± 0.51 (<i>p</i> < 0.001)	1.5

FIGURE CAPTIONS

Fig. 1. Map of the Inner, Middle and Outer Shelf of the Eastern Bering Sea off Alaska.

Fig. 2. Correlation coefficients between spatial variation in density and spatial variation in condition and between spatio-temporal variation in density and spatio-temporal variation in condition, predicted by the Akaike's information criterion (AIC)-selected spatio-temporal models. Error bars represent mean \pm standard error. *P*-values for a two-sided Wald test (strength-of-evidence measures of importance) are also indicated. KF = Kamchatka flounder (*Atheresthes evermanni*) – AF = arrowtooth flounder (*Atheresthes stomias*) – FS = flathead sole (*Hippoglossoides elassodon*) – YS = yellowfin sole (*Limanda aspera*) - PC = Pacific cod (*Gadus macrocephalus*) – WP = walleye pollock (*Gadus chalcogrammus*).

Fig. 3. Spatial variation (i.e. unmeasured variation that is stable over time) in (a) log-density and (b) log-condition, and spatio-temporal variation (i.e. unmeasured variation that changes between years) in (c, e) log-density and (d, f) log-condition for different years of the period 1992-2016, for the Akaike's information criterion (AIC)-selected model of Kamchatka flounder (*Atheresthes evermanni*). The color legends for spatio-temporal variation in log-density and log-condition are provided in the rightmost column and have units $\ln(\text{abundance} \cdot \text{km}^{-2})$ in the case of log-density and $\ln(g)$ in the case of log-condition.

Fig. 4. Spatial variation (i.e. unmeasured variation that is stable over time) in (a) log-density and (b) log-condition, and spatio-temporal variation (i.e. unmeasured variation that changes between years) in (c, e) log-density and (d, f) log-condition for different years of the period 1992-2016, for the Akaike's information criterion (AIC)-selected model of arrowtooth flounder (*Atheresthes stomias*). The color legends for spatio-temporal variation in log-density

and log-condition are provided in the rightmost column and have units $\ln(\text{abundance.km}^{-2})$ in the case of log-density and $\ln(g)$ in the case of log-condition.

Fig. 5. Spatial variation (i.e. unmeasured variation that is stable over time) in (a) log-density and (b) log-condition, and spatio-temporal variation (i.e. unmeasured variation that changes between years) in (c, e) log-density and (d, f) log-condition for different years of the period 1992-2016, for the Akaike's information criterion (AIC)-selected model of yellowfin sole (*Limanda aspera*). The color legends for spatio-temporal variation in log-density and log-condition are provided in the rightmost column and have units $\ln(\text{abundance.km}^{-2})$ in the case of log-density and $\ln(g)$ in the case of log-condition.

Fig. 6. Trends in relative abundance-weighted condition (grey line: mean; grey shading: 95% confidence interval) predicted by the Akaike's information criterion (AIC)-selected spatio-temporal models of the six study species. For each species, only predictions for those years where both density and length-weight data were available are shown. Relative abundance-weighted condition is abundance-weighted condition relative to mean abundance-weighted condition over the years for which both density and length-weight data were available.

FIGURES

Fig. 1

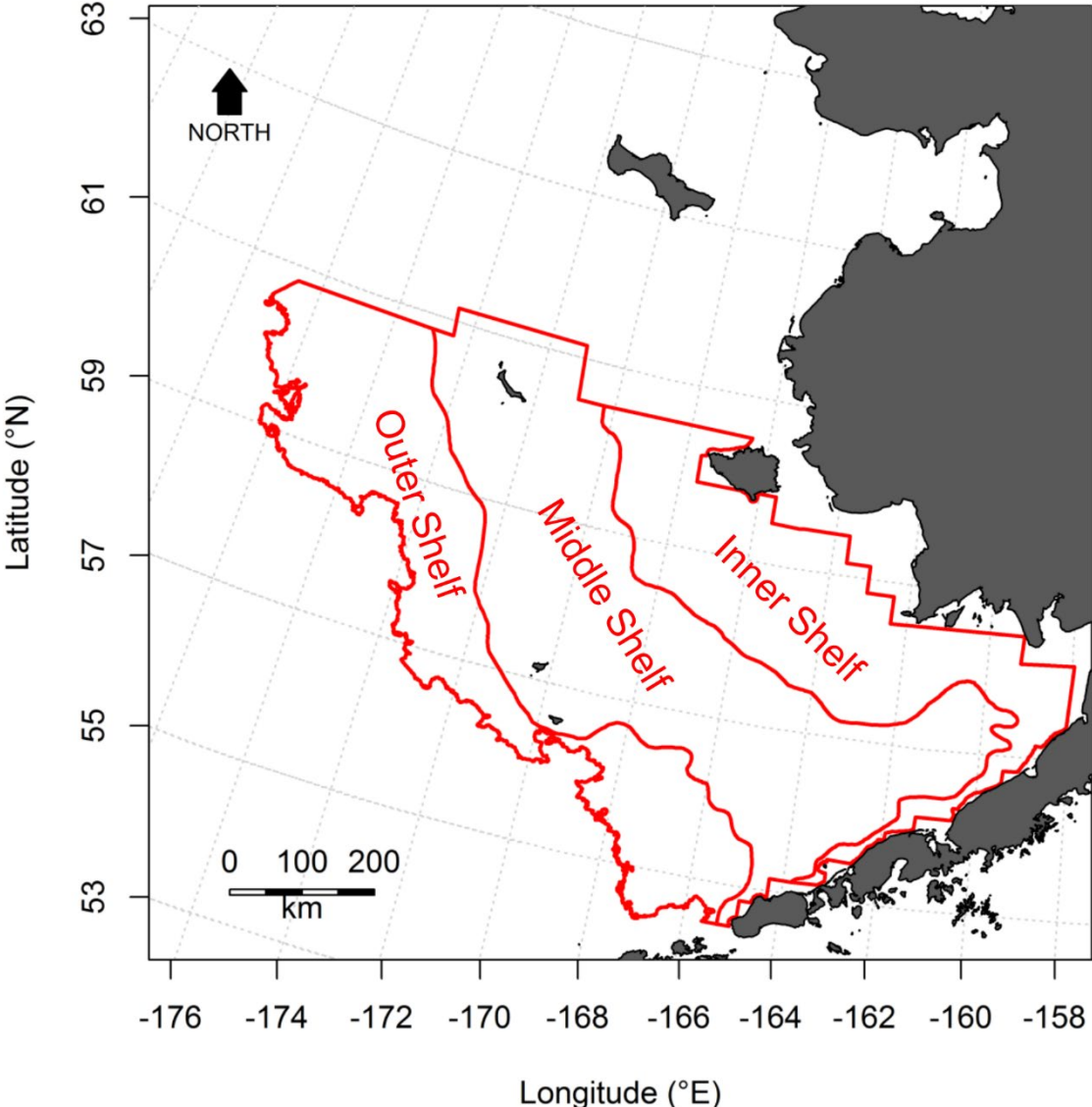


Fig. 2

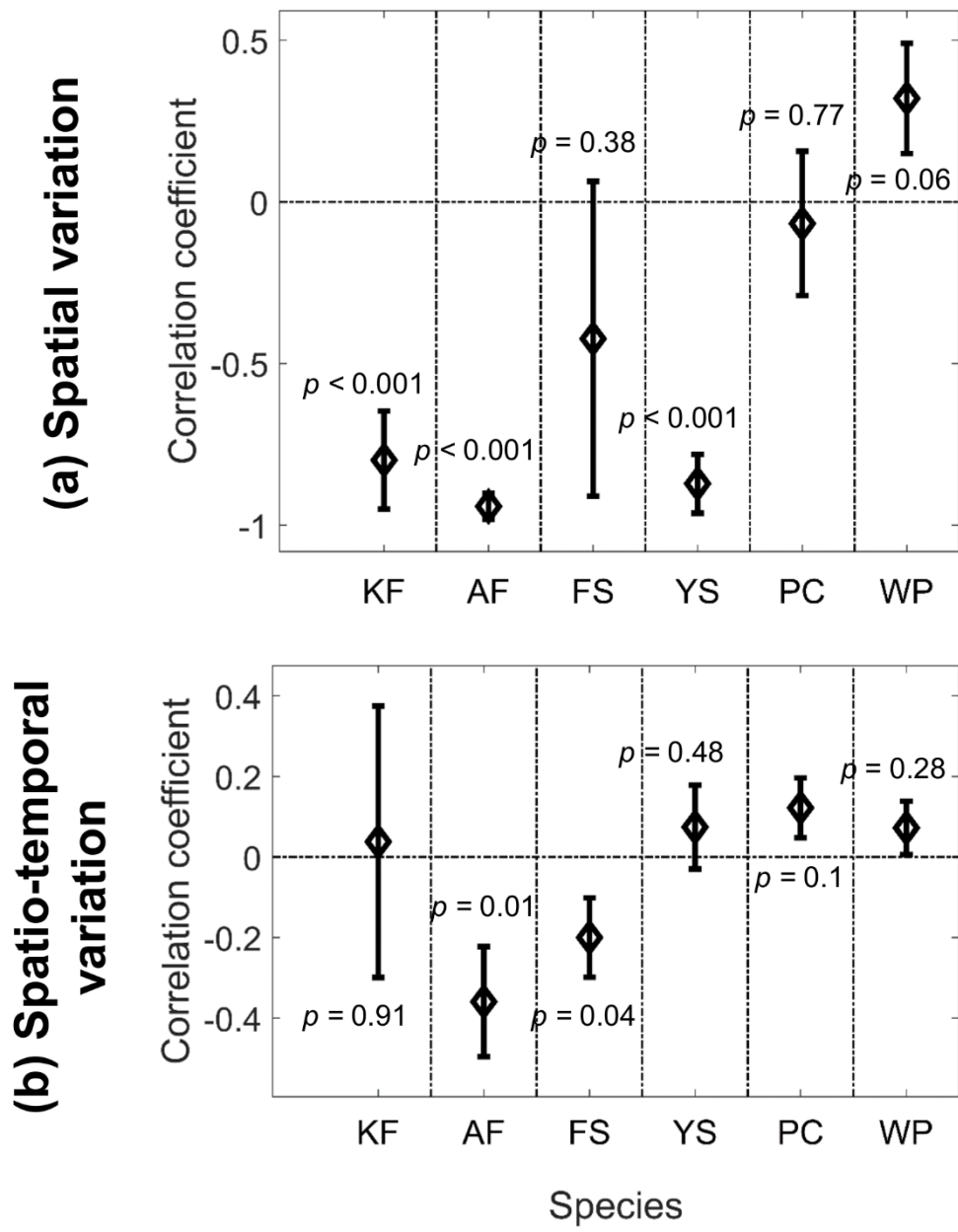


Fig. 3

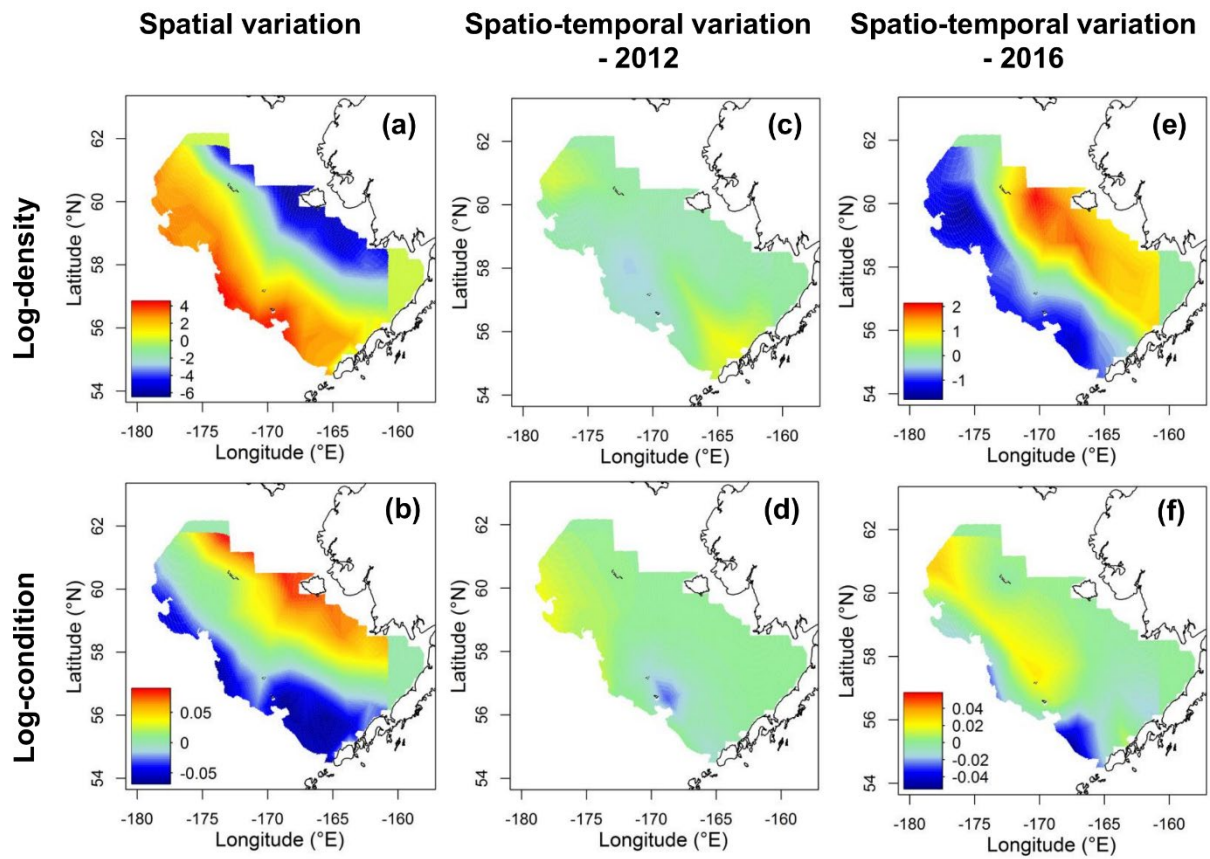


Fig. 4

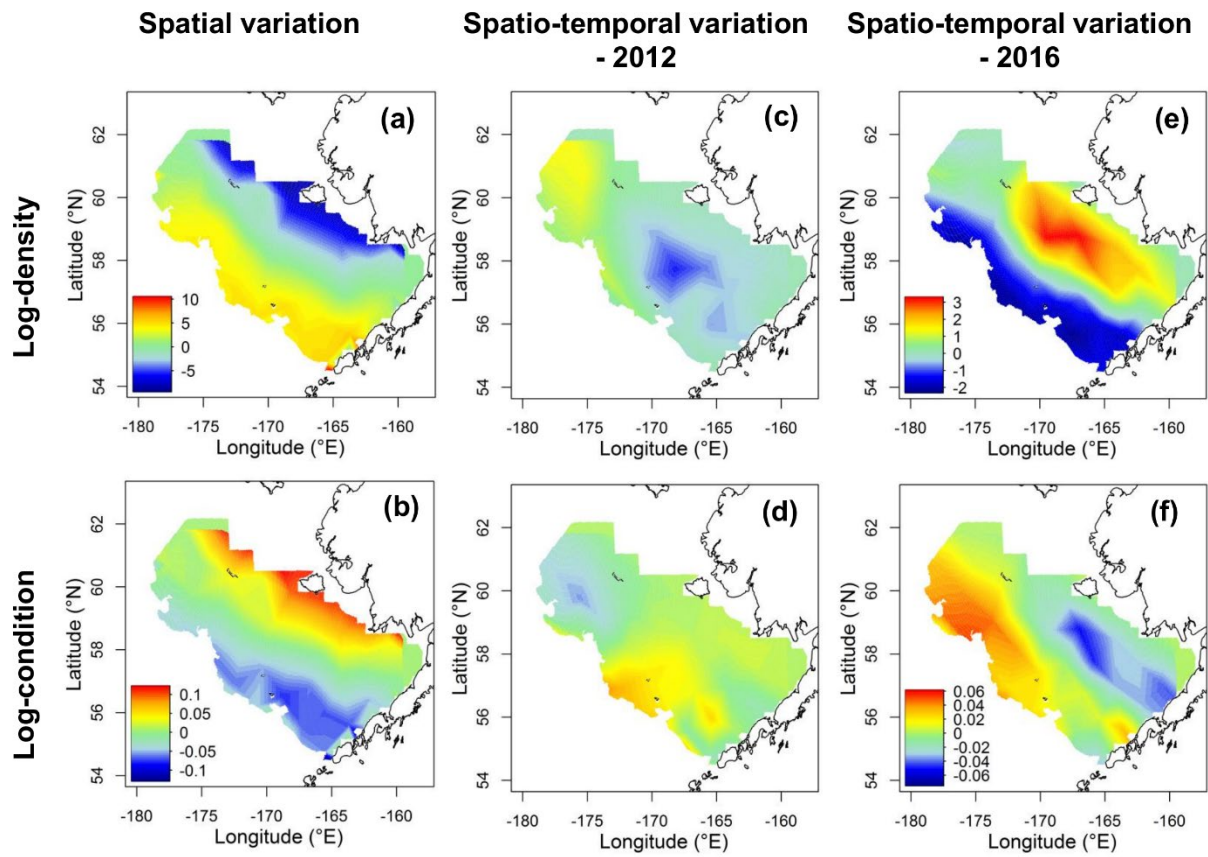


Fig. 5

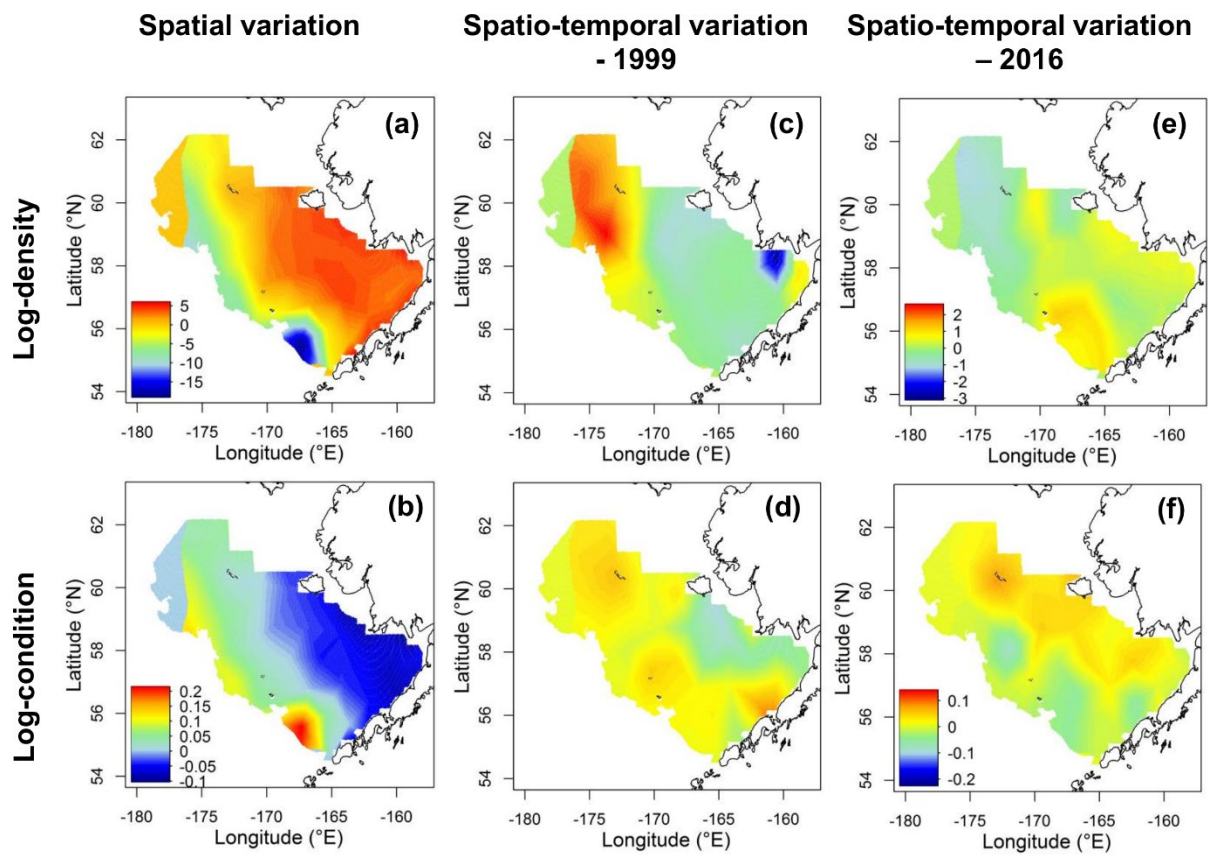


Fig. 6

